A Comprehensive Energy Model and Energy-Quality Evaluation of Wireless Transceiver Front-Ends

Y. Li, B. Bakkaloglu and C. Chakrabarti
Department of Electrical Engineering
Arizona State University
Tempe, AZ 85287-5706

Abstract—**As CMOS technology scales down, digital supply voltage and digital power consumption goes down. However due to dynamic range limitations, power supply and power consumption of the RF front-ends and analog sections do not scale in the same fashion. In fact, in scaled systems, the RF section of a wireless transceiver consumes more energy than the digital part. For better understanding of the design trade offs, we first develop an accurate and comprehensive energy model for the analog front-end of wireless transceivers. Next, we evaluate a single user point-to-point wireless data communication system and a multi-user CDMA based system with respect to RF front end energy consumption and communication quality. We demonstrate the effect of occupied signal bandwidth, peak-to-average ratio (*PAR*), symbol rate, constellation size, and pulse-shaping roll-off factor on single user system, and the effect of number of users and multiple access interference (MAI) on CDMA based multi-user system. For a given quality specification, we show how the energy consumption can be reduced by adjusting one or more of these parameters.**

1. INTRODUCTION

Wireless communication and mobile computing devices are widely used in everyday life. All of these devices are powered by a limited lifetime battery source. Since the advances in battery technology have failed to keep up with the battery capacity demands in mobile communications, aggressive techniques to reduce the power consumption of wireless communication devices have to be developed.

Different aspects of low power wireless communication have been addressed in recent years. These include the effect of modulation scaling [1], lazy packet transmission [2], energy efficient routing [3] etc. In these power analyses, the RF circuit energy is often ignored or over simplified. However, the RF section processes analog signal with higher frequency and consumes more energy than the digital part. To analyze RF circuit energy consumption, an accurate and comprehensive RF energy model is necessary.

Several transceiver energy models have been proposed in recent years. For microsensor systems, the transceiver energy model considers the circuit start-up energy in addition to steady state dissipated energy in [4]. The energy consumption of every component is assumed to be constant. Another high level model was proposed in [1], which divides the transceiver circuitry power into two parts, one related to the instantaneous symbol rate and the other to the highest symbol rate. This model is not comprehensive since the dissipated circuit power is related not only to the symbol rate, but also to parameters, such as peak-to-average ratio (*PAR*), required resolution in data converters, signal bandwidth, sampling frequency, etc. The energy model in [5] is more comprehensive but it also assumes a constant power value for most components and the power model for power amplifier is only gain dependent.

In this paper, we first present an accurate and comprehensive energy model for the RF front-end of a wireless transceiver. The components include ADC, DAC, reconstruction filter, mixer, frequency synthesizer, power amplifier, low noise amplifier (LNA) and baseband amplifier. We consider the effects of signal bandwidth, *PAR*, symbol rate, sampling frequency, constellation size, etc. on the power consumption of each of these components. We next study the role of *PAR* on the RF front-end energy consumption and symbol error rate (*SER*) for both single user and multi-user wireless communication systems. We show the effect of symbol rate, thermal noise, roll-off factor and the constellation sizes on the performance of a single user system. We also demonstrate the effect of MAI, roll-off factor and number of users on a CDMA based multi-user system.

The remainder of this paper is organized as follows. Section 2 describes the transceiver system model and defines the terminology used in this paper. Section 3 describes the power model for every component in the wireless transceiver. Section 4 describes the effect of design parameters such as *PAR* and signal bandwidth on the RF front-end energy consumption. Section 5 analyzes the communication quality of both single user wireless data transmission and multi-user CDMA system. Section 6 summarizes the paper.

2. SYSTEM MODEL FOR TRANSCEIVER

2.1 Transceiver Building Blocks

In order to minimize the total RF front-end energy consumption of a transceiver, it is essential to develop accurate energy models for all the key signal processing blocks. Since the RF and analog baseband section consumes majority of the total power, in this paper, we focus on developing power models for them. The wireless transmitter and receiver model that we have used is described in Fig. 1 and Fig. 2 [6]. The main components of the analog signal chain of the transmitter are DAC, reconstruction filter, mixer, power amplifier, RF filter. Similarly, the main components of the receiver signal chain are RF band select filter, LNA, baseband amplifier, baseband & anti-aliasing filter, ADC and RF synthesizer. The energy models for each of these components have been described in Section 3.

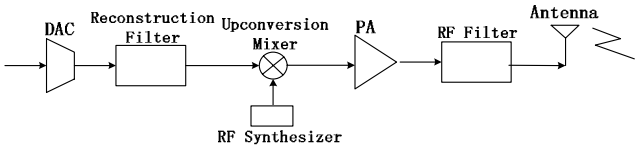

Fig.1 Block diagram of the transmitter analog signal chain

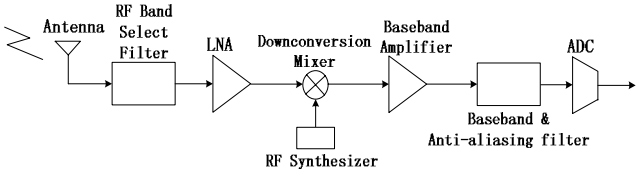

Fig.2 Block diagram of the receiver analog signal chain

2.2 Operation Modes for RF Transceivers

We assume that the transceiver works in three states: active state when the signal is transmitted, sleep state when there is no signal transmission, and transient state when the transceiver switches from sleep state to active state, and vice verse. The total energy consumption is given by

$$E_{total} = P_{on}T_{on} + P_{sleep}T_{sleep} + P_{transient}T_{transient}$$

In this paper we only consider active state power consumption. We divide the energy consumption in the active mode into two parts: signal transmission energy or radiated energy, which is delivered to the antenna, and dissipated energy which is the energy consumed by the electronic circuits. Since transmission energy is delivered by PA, P_{PA} includes both radiated energy and dissipated energy [5].

$$E_{active}=(P_{PA}+2P_{mix}+2P_{FS}+P_{LNA}+P_{filter}+P_{BA}+P_{DAC}+P_{ADC})T_{on} \quad (1)$$

where P_{PA}, P_{mix}, P_{FS}, P_{LNA}, P_{filter}, and P_{BA} are the power consumption of the PA, mixer, frequency synthesizer, low noise amplifier (LNA), filters and baseband amplifier (BA), respectively. The factor 2 before P_{mix} and P_{FS} comes from the assumption that the mixers and the frequency synthesizers have the same power consumption in both the transmitter and the receiver circuitry.

2.3 Performance Metrics

In this paper, we evaluate the performance of the wireless communication node with respect to energy consumption of the RF front-end and communication quality. We consider the effects of Bandwidth (BW), SNR (Signal-Noise-Ratio) and peak-to-average ratio (*PAR*). We evaluate the communication quality in terms of Symbol Error Rate (*SER*).

Noise figure is a measure of how much the SNR degrades as the signal passes through the signal chain [6]. $NF = SNR_{in}/SNR_{out}$ where SNR_{in} and SNR_{out} are the signal-to-noise ratios measured at the input and output points, respectively.

PAR is the ratio of signal peak power of the signal to its *rms* value. *PAR* gives information on how the signal is distributed over the amplitude range. A low *PAR* indicates a more uniform distribution, which is energy efficient. However, for single user and point-to-point wireless communication, lower *PAR* reduces communication quality.

There are several existing techniques to reduce the *PAR*, including clipping [7], block coding [8], use of companding transform [9], etc. However, if raised cosine pulse-shaping filter (which is typically placed before DAC in Fig. 1) is utilized, the values of *PAR* can also be changed by the roll-off factor of the filter. Since pulse-shaping filter is one of the basic blocks in most communication systems, this technique can be used on top of the existing techniques. The raised cosine filter in time-domain can be described by [10]

$$h(t) = \left(\frac{\sin(\pi t / T_s)}{\pi t}\right) \cdot \left(\frac{\cos(\pi\alpha t)}{1-(4\alpha t/(2T_s))^2}\right)$$

where *Ts* is the symbol rate and α is the roll-off factor.

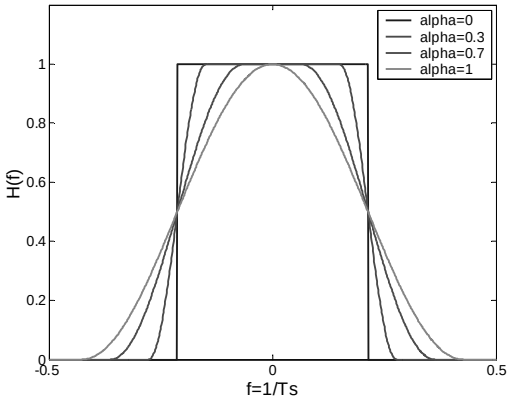

Fig.3 Frequency response of the pulse-shaping filter for different roll-off factors

Fig.3 describes the frequency response of the pulse shaping filter. From this figure, we can see that higher α value results in larger bandwidth. When $\alpha=0$, the frequency response is rectangular, the regrowth bandwidth is zero, and the *PAR* is the highest. When α increases, the regrowth bandwidth increases and the *PAR* reduces. So the roll-off factor can be used to control regrowth bandwidth and *PAR*.

3. POWER MODEL

In this section, we present the power models for each of the components in the analog signal chain of a transmitter/receiver. The existing power models for DAC [11], ADC [15] and class A PA [13] have been enhanced and new models have been developed for the PLL and VCO.

3.1 DAC Power Model

The digital to analog converter (DAC) converts the digital signal obtained at the output of the digital modulation blocks to analog signal. It is the first block in the analog signal chain of the transmitter.

We chose the current-steering DAC [11], which uses a number of binary scaled current source elements to generate the output voltage across a load resistor. The power consumption can be divided into two parts: the static power consumption P_s and the dynamic power consumption P_d. The dynamic power consumption is due to switching between symbols and is not considered here.

$$P_s = V_{dd} \cdot I_0 \cdot E\left[\sum_{i=0}^{N_1-1} 2^i \cdot b_i\right] = \frac{1}{2} V_{dd} \cdot I_0 \cdot (2^{N_1} - 1) \quad (2)$$

where b_i input digital bitstream, V_{dd} is the power supply and I_0 is the unit current source corresponding to b_0, the Least Significant Bit (LSB). I_0 is a constant value for a given hardware technology and we assume $I_0 = 5\ uA$ in the following simulation. So P_s is only decided by the resolution of DAC.

The resolution N_1 can be expressed in terms of DAC SNR and signal *PAR* as in [11]

$$N_1 = \frac{SNR + PAR - 4.77\,dB}{6.02} \quad (3)$$

P_{DAC} can then be expressed as a function of *PAR*.

$$P_{DAC} = 0.5 \cdot V_{dd} \cdot I_0 \cdot \left(2^{SNR+PAR-4.77\,dB/6.02} - 1\right) \quad (4)$$

3.2 Analog filter power model

The output of the DAC is fed to the reconstruction filter in the transmitter. The reconstruction filter suppresses the Nyquist images due to zero order hold (ZOH) operation of the DAC. The digital pulse shaping filter precedes the DAC and it can adjust the peak-to-average ratio and excess bandwidth of transmission signals. The RF filter at the output of the PA helps with suppression of spurious emissions and thermal noise floor from transmitter circuitry. At the receiver, the RF band select filter suppresses wideband interference signals and helps with the linearity of the receiver. Baseband filters suppress in-band interference and help with anti-aliasing filtering for the ADC.

We can estimate baseband active analog filter power consumption as follows [12]

$$P_{filter} = n \cdot kT \cdot Q \cdot f_0 \cdot SNR^2 \quad (5)$$

where n depends on the filter topology, the active elements used (op-amp RC, transconductance-C, etc). Further, Q is the quality factor, f_0 is the center frequency (bandpass filter), and SNR is the signal-to-noise ratio of the filter.

3.3 Frequency Translation Circuits

Mixers are commonly used for frequency translation (upconversion and downconversion) in RF transceivers. This frequency translation is a result of time-domain multiplication of high frequency input signal (RF input) with a spectrally clean local oscillator (LO) signal. LO signal is generated by a phase-locked loop (PLL) synthesizer coupled with a voltage controlled oscillator (VCO).

3.3.1 PLL Power Consumption

The most critical building blocks that consume quiescent current for an integer-N PLL frequency synthesizer is the multi-modulus feedback divider (MMD) and phase-frequency detector (PFD). For narrowband communication systems, where RF center frequency F_{LO} is much higher than the occupied bandwidth of the modulated signal BW, the power consumption of a integer-N PLL, with frequency multiplication ratio of N can be estimated as follows:

$$P_{pll} = b_1 \cdot C_1 \cdot V_{dd}^2 \cdot F_{LO} + b_2 \cdot C_2 \cdot V_{dd}^2 \cdot F_{ref} \quad (6)$$

where b_1 and b_2 are proportionality constants, C_1 and C_2 is the total parasitic capacitance loading of the RF circuits, F_{ref} is the reference frequency and V_{dd} is the supply voltage, which is also assumed to be equivalent to the LO voltage swing.

3.3.2 VCO Power Consumption

VCO phase noise determines the far-out phase noise of LO signal and it has direct impact on receiver noise figure (NF) and transmit signal quality (EVM/SNR/transmit signal mask). Low power and low phase noise is a conflicting requirement for RF VCOs. An RF oscillator consists of a parallel resonant tank built by an inductor L, capacitor C, with an active element denoted by negative resistance –R compensating for tank losses. Voltage dependent capacitor C (varactor) tunes the center frequency of the VCO yielding $\omega_c = 1/\sqrt{LC}$. The power loss in the tank resistor is calculated as:

$$Pvco = C\frac{R}{L}V^2{}_{pk} = RC^2\omega_c{}^2 V_{pk}{}^2 = \frac{R}{L^2\omega_c{}^2} V_{pk}{}^2 \quad (7)$$

where V_{pk} and I_{pk} is the peak voltage and current amplitude inside the tank circuit. The power consumption of VCOs decrease linearly with lower series resistance in the tank and increases with peak signal swing.

3.4 Mixer and LNA power model

There are two mixers in the transceiver. Upconversion mixer in the transmitter moves the baseband signal to a higher frequency. The downconversion mixer in the receiver demodulates the RF signal from RF to baseband.

The power model of the mixer is a function of the noise figure *NF* and the gain *K*.

$$P_{mixer} = k_{mixer} \cdot K / NF \quad (8)$$

LNA (Low-Noise-Amplifier) amplifies the received signals with low input referred noise. LNA determines the overall noise figure of the receiver. Similar to mixer, for a low-noise amplifier, the power consumption P_{LNA} is a function of the noise figure *NF* and the gain *A*. LNA power model can be described as

$$P_{LNA} = k_{LNA} \cdot A / NF \quad (9)$$

3.5 Power Amplifier Model

The power amplifier (PA) boosts the signal power so that the antenna can radiate sufficient power for reliable communication. We choose Class A PA since we consider MQAM in our analysis and simulation of point-to-point communication and PSK for CDMA based communication. The high linearity of this amplifier preserves communication accuracy and limits spectral regrowth. We describe a practical Class A PA energy model below.

The drain efficiency, η, of Class A PA is proportional to the output power [13].

$$\eta = \frac{P_{out}}{P_{PA}} = \frac{P_{out}}{P_{out\_\max}} \cdot K \quad (10)$$

where P_{out} is the output power, P_{out_max} is the peak value of P_{out} and K is a constant. We choose *K=0.5* in our simulation. P_{out_max} is also a function of the *rms* value of power $P_{rms,}$ and the peak-to-average ratio, *PAR*. P_{rms} is proportional to the received signal power $P_{received}$, the antenna gain, the propagation distance

and P_{PA}. According to [10], the symbol error rate at the receiver can be expressed as

$$SER = 4\left(1-\frac{1}{\sqrt{M}}\right)\cdot Q\left(\sqrt{\frac{3\cdot P_{received}}{(M-1)\cdot N}}\right) \quad (11)$$

where N is the noise power, M is the constellation size. So

$$P_{received} = \frac{1}{3}(2^b-1)\cdot N\cdot\left(Q^{-1}\left(\frac{1}{4}\left(1-\frac{1}{2^{b/2}}\right)^{-1} SER\right)\right)^2$$

Assume free space propagation at distance d (meter). G_t and G_r is the transmitter and receiver antenna gain, L is the system loss factor not related to propagation, λ is the carrier wavelength. PA is given by

$$P_{PA} = \frac{16\cdot\pi^2\cdot d^2\cdot L}{3G_rG_t\lambda^2\cdot K}(2^b-1)\cdot N\cdot\left(Q^{-1}\left(\frac{1}{4}\left(1-\frac{1}{2^{b/2}}\right)^{-1} SER\right)\right)^2 PAR \quad (12)$$

For other modulation scheme, the PA power model is similar but the Q function is different.

3.6 Baseband Amplifier Power Model

After downconversion, an IF (or baseband) low-noise amplifier is used to provide gain for signal before A/D conversion. Larger signal amplitudes give a higher SNR in the ADC and improve the receiver BER. Depending on the receiver linearity requirements, multiple filter and gain stages may be necessary to suppress in-band interferers. As shown in [14], power consumption of baseband amplifier is proportional to the gain and the bandwidth.

$$P_{BA} = k\cdot 2B\cdot\sqrt{a_{BA}}$$

where the coefficient $k=2.45x10^{-13}$ *W/Hz* is decided by device dimensions and other process parameters. a_{BA} is the baseband amplifier gain that is assumed to be $a_{BA}=2$.

3.7 ADC Power Model

Analog-to-digital converter (ADC) converts the baseband analog signal to the baseband digital signal in the receiver.

If Nyquist-rate ADC is used in the transceiver, we can use an accurate power estimation model from [15]. The power consumption of ADC can be calculated as follows

$$P_{ADC} = \frac{V_{dd}^2\cdot L_{\min}\cdot(f_{sample}+f_{signal})}{10^{(-0.1525\cdot N_1+4.838)}}$$

where N_1 is the resolution of A/D converter (see Eqn.3), L_{min} is the minimum channel length for the given CMOS technology and equals 0.4 *um*. V_{dd} is equal to *3V*.

4. FRONT-END ENERGY CONSUMPTION EVALUATION

In this section, we study the effect of *PAR* on the front-end energy consumption. We use the single user wireless communication system that uses MQAM as an example. Note that although CDMA system works on a higher frequency and wider band, the effect of *PAR* on the front end energy is similar.

4.1 Effect of PAR on Energy Consumption

Table 1 summarizes the related parameters for the power consumption of different components in RF front-ends. From Table 1, we see that the power consumption of PA, ADC and DAC is function of the *PAR*, while the power consumption of filters, mixer, frequency synthesizer, LNA and baseband amplifier is not affected by *PAR*. We take two values of *PAR:* 3 *dB* and 10 *dB* as examples. We see that while the PA power is less dominant at lower *PAR*, it is by far the largest component for high *PAR*.

	Power Model Function	*PAR=10dB*	*PAR=3dB*
PA	*P(PAR, d, b, SER)*	*246 mW*	*47.88 mW*
Mixer	*P(K,NF)*	*30.3mW*	*30.3mW*
FS	$P(\omega_c, F_{LO}, F_{ref})$	*67.5mW*	*67.5mW*
LNA	*P(A, NF)*	*20mW*	*20mW*
ADC	*P(PAR, SNR, f)*	*5.85mW*	*3.89mW*
DAC	*P(PAR,SNR)*	*2.43mW*	*1.08mW*
Filter	*P(f, SNR)*	*5mW*	*5mW*
BA	$P(B, \alpha_{BA})$	*5mW*	*5mW*

Table 1 RF power consumption for different blocks in a transceiver; P_{rms}=12 mW

In the rest of this section, we evaluate the energy performance of the system with respect to the active RF front-end energy per bit, E_{bit}.

$$E_{bit}=(P_{non\text{-}PAR}+P_{PAR})T_{bit}=(P_{non\text{-}PAR}+P_{PAR})/(R_sb) \quad (14)$$

where R_s is the symbol rate and b is the number of bits in one symbol ($b=log\ M$).

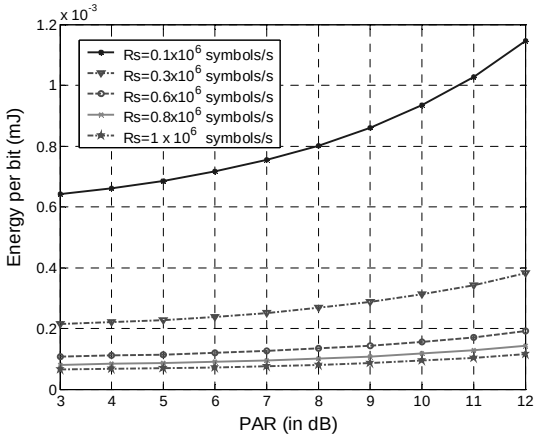

Fig.5 16 QAM energy consumption per bit for different values of *PAR*; transmission power P_{rms}=12 mW

Fig.5 shows the effect of *PAR* and the symbol rate on the active RF front-end energy per bit, E_{bit}, for b=16. For fixed R_s and fixed *b (bits/symbol)*, E_{bit} increases with *PAR*. This is because the power of PA, ADC and DAC increases with *PAR* (Table 1). If we further fix *PAR* and compare E_{bit} for different symbol rates, we can see that higher the symbol rate, the lower the energy consumption. This is because higher symbol rate results in shorter bit duration ($T_{bit}\propto 1/R_s$). Thus for 16QAM, E_{bit} can be reduced by operating the system at low *PAR* and/or high symbol rates. If the symbol rate is low, it is even more important that the *PAR* be kept as low as possible.

Next, we compare the effect of *b*, the number of bits per symbol (for a fixed symbol rate R_s), on E_{bit}. While the PA energy consumption increases with both transmission distance and *b* (*bits/symbol*) (see Eqn.12), the active energy of other

components is inversely proportional to *b* (see Eqn.14). For small values of *b*, PA energy consumption is low and E_{bit} reduces with increase in *b (bits/symbol)*. For higher *b (bits/symbol)*, PA energy consumption becomes dominant and E_{bit} increases. We demonstrate this in Fig.6 for transmission distance *d=1m*. We consider the relation between E_{bit} and *b (bits/symbol)* for different *PAR*. For a specific value of *PAR*, there is an optimal value of *"b" (bits/symbol)* for which E_{bit} is the minimum. Also, as *PAR* increases, the optimal value of *b* reduces. This is because as *PAR* increases, the PA energy becomes dominant for lower value of *b (bits/symbol)*.

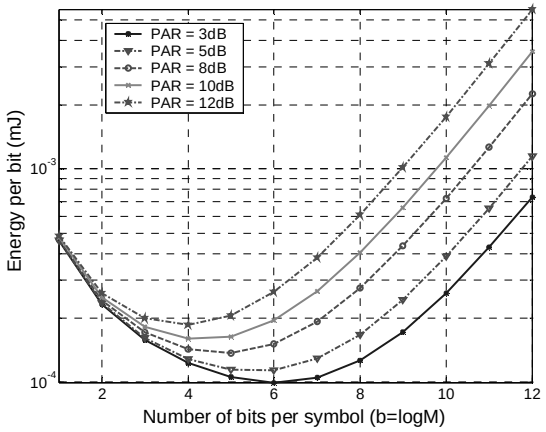

Fig.6 Energy consumption of RF front-end for different *b (bits/symbol), d=1m,* $R_s = 0.5MHz$

As the transmission distance increases, the optimal *b (bits/symbol)* corresponding to minimum E_{bit} also reduces. This is because as the distance increases, the effect of PA energy increases. For large distances, the PA energy is significantly larger and PA energy becomes dominant for smaller *b (bits/symbol)*.

5. COMMUNICATION QUALITY EVALUATION

In this section, we evaluate the communication quality (*SER*) of a point-to-point wireless data communication system and a multiple-user CDMA system. Although the RF transceiver front-ends are similar, the dominant cause of interference in the two systems is different. For point-to-point communications, thermal noise is dominant while for the CDMA system, multiple access interference (MAI) from other users (especially when the number of users is high) is dominant.

5.1 Effect of PAR on Thermal Noise Limited System

In this section, we describe the effect of *PAR* on the symbol error rate (*SER*) of a point-to-point wireless data communication system. For high data rate transmission, we assume MQAM is used.

From Section 2.3, we know that *PAR* can be adjusted by changing the roll-off factor α of the pulse shaping filter. Note that α changes the signal bandwidth by a factor of $(1+\alpha)$ [15]. If we choose the bandwidth of the low pass filter in the receiver to be the same as that of the signal and keep the received signal power, the noise power equals

$$N = 2B\sigma^2 \cdot NF = 2R_s(1+\alpha)\cdot\sigma^2 \cdot NF \qquad (15)$$

where σ^2 is the single-sided noise power spectral density and *NF* is the noise figure. Combining Eqn.11 and 15, we have

$$SER = 4(1-\frac{1}{\sqrt{M}})\cdot Q\left(\sqrt{\frac{3\cdot P_{received}}{(M-1)\cdot 2R_s(1+\alpha)\cdot\sigma^2\cdot NF}}\right)$$

Assuming $SNR_0 = \frac{P_{received}}{2R_s\sigma^2\cdot NF}$, then

$$SER = 4\left(1-\frac{1}{\sqrt{M}}\right)\cdot Q\left(\sqrt{\frac{3\cdot SNR_0}{(M-1)\cdot(1+\alpha)}}\right) \qquad (16)$$

Eqn.16 establishes the relationship between *SER* and the roll-off factor α. Fig.7 shows how *SER* increases with the increase in roll-off factor α for different constellation sizes, *M*=8, 16, 32. The increase in *SER* can be explained by the following: the increase in α expands the signal bandwidth and makes the noise power increase. Fig.7 also demonstrates the effect of α on the *PAR*. For a given M, as α increases, *PAR* reduces causing E_{bit} to reduce as well (see Fig.7).

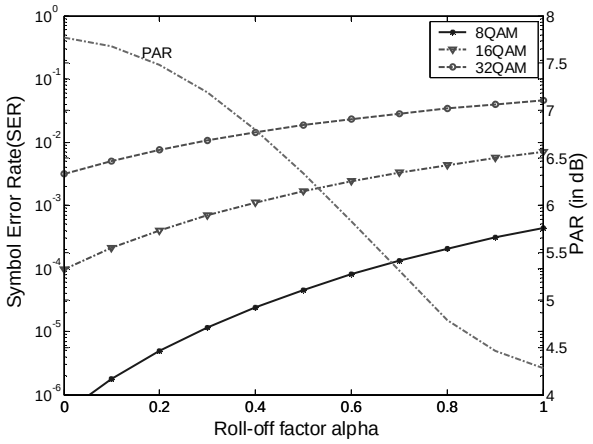

Fig.7 MQAM system: *SER* and *PAR* vs α, *d=1m*.

The above analysis can be used to design a low power system with given *SER* specification. From Fig.7, we can find multiple combinations of roll-off factor α and constellation size *M* that satisfy the *SER* requirement. For each combination (α, *M*), we can also find (*PAR*, *M*) from Fig.7. Next, we use Fig.6 to determine the active energy per bit, E_{bit}, for each candidate (*PAR*, *M*), and then choose the one with minimum E_{bit}. Thus we can determine the roll-off factor α and *b (bits/symbol)* corresponding to the minimum energy configuration for a given *SER*. Note that the minimum energy configuration changes with distance *d*.

5.2 Effect of PAR on CDMA System

In this section, we study the effect of *PAR* on a CDMA system where exist both MAI and thermal noise interference. We assume BPSK modulation is used here.

In this simulation, we choose the standard Gaussian approximation (SGA) [16] [17] to evaluate *SER*. According to SGA, MAI is modeled as a zero-mean Gaussian *RV*

$M \sim N[0, Var(M)]$ [18] and the probability of bit error rate (for BPSK, *BER* = *SER*) of any user can be expressed as

$$SER = Q\left(\left[\frac{1+\alpha}{2 \cdot SNR_0} + \frac{K-1}{2 \cdot PN}\left(1-\frac{\alpha}{4}\right)\right]^{-\frac{1}{2}}\right) \qquad (17)$$

where *K* is the number of users for in the system and *PN* is the length of spread spectrum sequence. Note that the first item in Q function is due to the AWGN channel and the second item due to MAI.

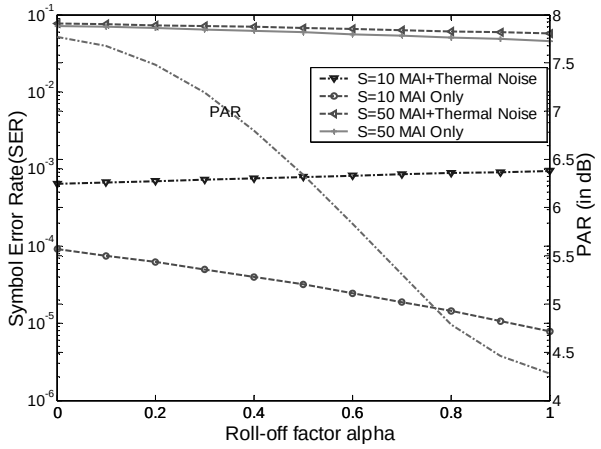

Fig.8 CDMA system: *SER* and *PAR* vs α , *PN=63*

Fig.8 describes how SER changes with roll-off factor α as the number of users in the system changes. It also shows the effect of MAI and thermal noise on SER for different number of users. For a CDMA based multi-user system with fixed roll-off fact α , as the number of users increase, the communication quality due to MAI deteriorates. When the number of users is more than 10, MAI is dominant and SER reduces with the increase in roll-off factor α . For instance, if the number of users is 50, SER reduces from 0.0734 for $\alpha = 0.2$ to 0.0654 for α =0.6. The reduction is because lower PAR (corresponding to greater α) introduces less MAI interference to other users in the same system -- a trend that has also been demonstrated in [16] [17]. However, when the number of users is low (less than 10), MAI is not as important as thermal noise and SER increases with roll-off factor α (blue dashed line in Fig.8). This trend is similar to that of point-to-point communication (Section 4.2). However if only MAI is considered for such a system (green dashed line in Fig. 8), we would conclude that SER reduces with α, which is not correct.

6. CONCLUSION

In this paper, we develop an accurate and comprehensive energy model for the RF front-end of a wireless transceiver. We consider the effects of signal bandwidth, *PAR*, symbol rate, modulation order *b (bits/symbol)*, transmission distance etc. on the total RF front-end energy consumption. For single user systems, we present a detailed study on the effect of *PAR* on the front-end energy consumption and symbol error rate (*SER*). For multi-user CDMA based systems, we show that the effect of *PAR* on overall front-end energy consumption is similar but the *SER* is different because of MAI.

Acknowledgement: This work was funded in part by the NSF I/UCRC center, Connection One (EEC-0226846), the NSF S/I/UCRC center, CLPE (EEC-9523338), and an NSF ITR (0325761).

7. REFERENCES

[1] C. Schurgers, M. B. Srivastava, etc., "Modulation scaling for energy aware communication systems," *ISLPED01*, Aug. 2001.

[2] B. Prabhakar, E. U. Biyikoglu and A. E. Gamal, "Energy efficient transmission over a wireless link via lazy packet scheduling," *IEEE INFOCOM* 2001.

[3] R. Ramanathan and R. Rosales-Hain, "Topology control of multihop wireless networks using transmit power adjustment," *Proc. IEEE INFOCOM*, 2000.

[4] A. Y. Wang, S. Cho, etc., "Energy efficient modulation and MAC for asymmetric RF microsensor system," *ISLPED01*, Aug. 2001.

[5] S. Cui, Ahmad Bahai, etc., "Modulation optimization under energy constraints," *IEEE International Conference on Communications, ICC 2003*, May 2003.

[6] B. Razavi, *RF microelectronics*, Prentice Hall, 1998.

[7] X. Li and L. J. Cimini, "Effects of clipping and filtering on the performance of OFDM," *IEEE Communication Letters*, Vol.2 No.5, pp.131-133, May 1998.

[8] T. A. Wilkinson and A. E. Jones, " Minimization of the peak to mean envelop power ratio in multicarrier transmission schemes by blocking coding," *Proc. IEEE VTC*, 1995, pp. 825-831, July, 1999

[9] X. Wang, T. T. Tjhung and C. S. Ng., "Reduction of peak-to-average power ratio of OFDM system using a companding technique," *IEEE Trans. On Broadcasting*, Vol. 45, No.3, pp. 303-307, September 1999.

[10] T. S. Rappaport, *Wireless communications principles and practice*, Prentice Hall, 1996.

[11] M. Gustavsson, J. J. Wikner and N. N. Tan, *CMOS data converters for communications*, Kluwer Academic Publishers, 2000.

[12] Y. P. Tsividis "Integrated continuous-time filter design—an overview," *IEEE journal of Solid-State Circuits*, Vol. 29, No.3, pp. 166-176, March 1994.

[13] P. F. Chen, L. E. Larson, etc., "High-efficiency power amplifier using dynamic power-supply voltage for CDMA applications," *IEEE transactions on microwave theory and techniques*, vol.47, Aug. 1999.

[14] T. H. Lee, *The design of CMOS radio-frequency integrated circuits*. Cambridge Univ. Press, Cambridge, U.K., 1998.

[15] E. Lauwers and G. Gielen, "Power estimation methods for analog circuits for architecture exploration of integrated systems," *IEEE transactions on VLSI systems*, vol. 10, No.2, April 2002.

[16] Y. C. Yoon, "A simple and accurate method of probability of bit error analysis for asynchronous band-limited DS-CDMA systems," *IEEE transactions on Communications*, Vol. 50, No.4, pp. 656-663, April 2002.

[17] Y. Asano, Y. Daido, etc., "Performance evaluation for band-limited DS-CDMA communication system," *IEEE VTC 1993*, May 1993.

[18] A. J. Viterbi, *CDMA: Principle of Spread Spectrum Communication*. Reading, MA: Addison-Wesley, 1995.